The Complete Nucleotide Sequences of the 5 Genetically Distinct Plastid Genomes of *Oenothera*, Subsection *Oenothera*: II. A Microevolutionary View Using Bioinformatics and Formal Genetic Data

Stephan Greiner,[*1] *Xi Wang,*[†1] *Reinhold G. Herrmann,*[*] *Uwe Rauwolf,*[*] *Klaus Mayer,*[†] *Georg Haberer,*[†] *and Jörg Meurer*[*]

*Lehrstuhl für Botanik, Department Biology I, Botany, Ludwig-Maximilians-University, Munich, Germany; and †MIPS/IBI Institute for Bioinformatics and Systems Biology, Helmholtz Center Munich; German Research Center for Environmental Health GmbH, Neuherberg, Germany

A unique combination of genetic features and a rich stock of information make the flowering plant genus *Oenothera* an appealing model to explore the molecular basis of speciation processes including nucleus–organelle coevolution. From representative species, we have recently reported complete nucleotide sequences of the 5 basic and genetically distinguishable plastid chromosomes of subsection *Oenothera* (I–V). In nature, *Oenothera* plastid genomes are associated with 6 distinct, either homozygous or heterozygous, diploid nuclear genotypes of the 3 basic genomes A, B, or C. Artificially produced plastome–genome combinations that do not occur naturally often display interspecific plastome–genome incompatibility (PGI). In this study, we compare formal genetic data available from all 30 plastome–genome combinations with sequence differences between the plastomes to uncover potential determinants for interspecific PGI. Consistent with an active role in speciation, a remarkable number of genes have high *Ka*/*Ks* ratios. Different from the Solanacean cybrid model *Atropa*/tobacco, RNA editing seems not to be relevant for PGIs in *Oenothera*. However, predominantly sequence polymorphisms in intergenic segments are proposed as possible sources for PGI. A single locus, the bidirectional promoter region between *psb*B and *clp*P, is suggested to contribute to compartmental PGI in the interspecific AB hybrid containing plastome I (AB-I), consistent with its perturbed photosystem II activity.

Introduction

The evolution of eukaryotic genomes originated in endosymbiotic cell conglomerates and was based on a conversion and an extension of the genetic potentials of initially free-living partner cells that coevolved into a single, integrated compartmentalized genetic system. To date, this machinery, with nucleus/cytosol and mitochondria in animals and fungi, and in addition with plastids in plants, is regulated spatiotemporally and quantitatively in its entirety. Mitochondria and chloroplasts possess only rudimentary genomes because they have lost a large fraction of their ancestral genes many of which by transfer to the nucleus (summarized in Herrmann [1997]; Martin et al. [1998]; Martin [2003]). However, much of the nuclear coding potential, in the order of 25–30%, is required for the management of the energy-transducing organelles (Herrmann 1997). This illustrates both their tight genetic and metabolic integration and the importance of the compartmentalized genetic system in the control of the principal energy supply for the cell. Coevolution of the intracellular genetic compartments can affect eukaryotic evolution on long and short timescales (Herrmann and Westhoff 2001; Herrmann et al. 2003). In the latter case, it becomes obvious after interspecific organelle exchanges, for example, of plastids and nuclei, that even between closely related species frequently cause serious disturbances in the development of the resulting cybrids or hybrids (Stubbe 1989; Schmitz-Linneweber et al. 2005). Compartmental coevolution is characteristic of eukaryotic organisms and an important, often neglected, element in speciation processes (Levin 2003).

Over the past century, the Onagracean genus *Oenothera* has developed as a model for studying plant evolution and represents an ideal taxon for application of modern molecular genetic strategies to elucidate mechanisms of speciation including aspects of the compartmentalized genetic machinery, notably of plastids. The genus represents a well-defined group of flowering plants, presumably the best-known plant taxon of its size (Raven 1988; Levin et al. 2003, 2004), for which a rich stock of biosystematic, taxonomic, and genetic information is available. *Oenothera* genetics includes a unique combination of features, such as biparental transmission of plastids, a general interfertility of species, viable and fertile hybrid offspring, as well as permanent translocation heterozygotic genomes, generally operating in combination with a system of gametophytic or sporophytic lethal factors. Together they allow the exchange of plastids and nuclei as well as the substitution of entire haploid chromosome sets or of individual (or more) chromosome pairs between species. Such exchanges frequently result in developmentally impaired, though fertile, plastome–genome incompatible hybrids (Cleland 1972; Stubbe and Raven 1979; Stubbe 1989; Harte 1994; Dietrich et al. 1997). Initially, *Oenothera* research was focused predominantly on an understanding of the nuclear genome, particularly of the phenomenon of translocation heterozygosity, its nature, origin, patterns, and impact for speciation (summarized in Cleland [1972]; Harte [1994]). The crucial role of the plastome in the evolution of the genus has become obvious since Renner's (1934) fundamental genetic work. Together, these studies resulted in a greater insight into both the evolutionary structure and dynamics of the clade (Stubbe 1964; Cleland 1972; Stubbe and Raven 1979; Harte 1994; Dietrich et al. 1997).

Subsection *Oenothera* (=*Euoenothera*) is 1 of the 5 subsections of the section *Oenothera* on which most of the experimental work on evolution in this taxon has been

[1] These authors contributed equally to this work.

Key words: *Oenothera* chloroplast genome, cytonuclear coevolution, interspecific plastome–genome incompatibility, speciation, Dobzhansky–Muller incompatibility, microevolution.

E-mail: joerg.meurer@lrz.uni-muenchen.de.

Mol. Biol. Evol. 25(9):2019–2030. 2008
doi:10.1093/molbev/msn149
Advance Access publication July 8, 2008

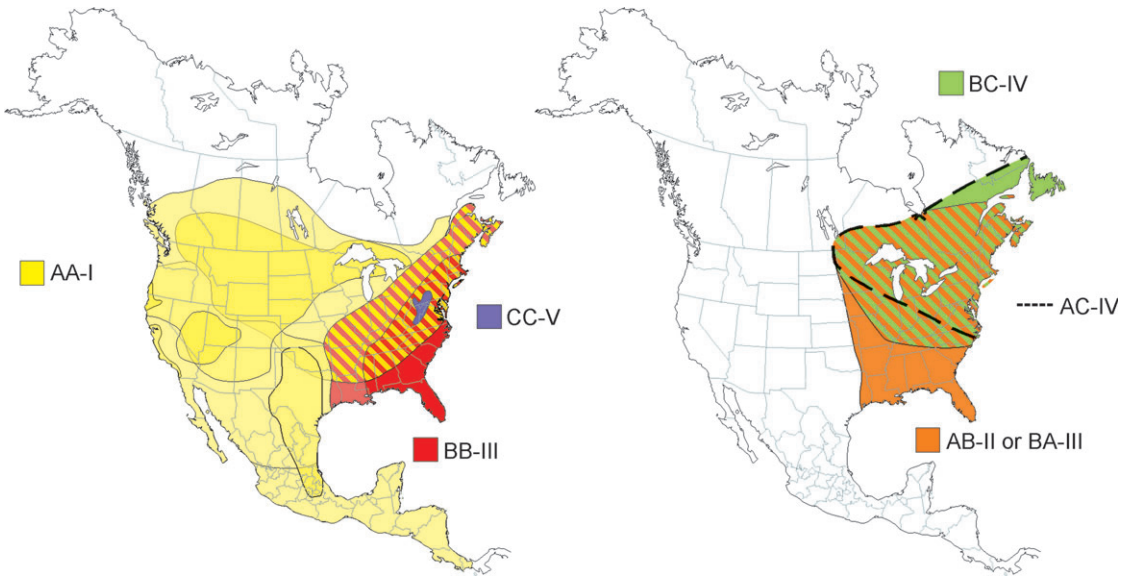

FIG. 1.—Distribution of the 11 North American species of subsection *Oenothera* of the genus *Oenothera*. The map summarizes data presented in Dietrich et al. (1997) and includes information about the 6 basic nuclear genotypes containing the 3 haploid genomes, A, B, and C, and their associated plastome types (I–V) of that subsection. Yellow and red gradations designate the distribution of distinct AA-I and BB-III genotypes. The left map shows the areas populated by homozygous species, the right one that of their hybrids. Note that all genotypes overlap geographically.

performed. It is comprised of somewhat more than a dozen species with numerous variants (Dietrich et al. 1997). Their genotypes, 3 basic genomes (A, B, and C) in homozygous (AA, BB, CC) or heterozygous (AB, AC, BC) constitution associated with 5 genetically distinguishable plastomes (I–V) in distinct combinations, and habitats are well definable. Although all these species overlap geographically (fig. 1), are interbreeding, and their hybrids are fully fertile, the subsection has been convincingly demonstrated to represent a natural group of closely related species that can unambiguously be discerned morphologically, cytogenetically, and in particular on the basis of their relationships between their genomes and plastomes (Stubbe 1964; Dietrich et al. 1997; fig. 2).

To obtain a more precise understanding of speciation processes including the entire compartmentalized plant genome and of the taxonomic and evolutionary relationships of the species involved, we generated and applied an EST library, developed molecular markers of the nuclear and plastid genomes of subspecies for genotyping approaches

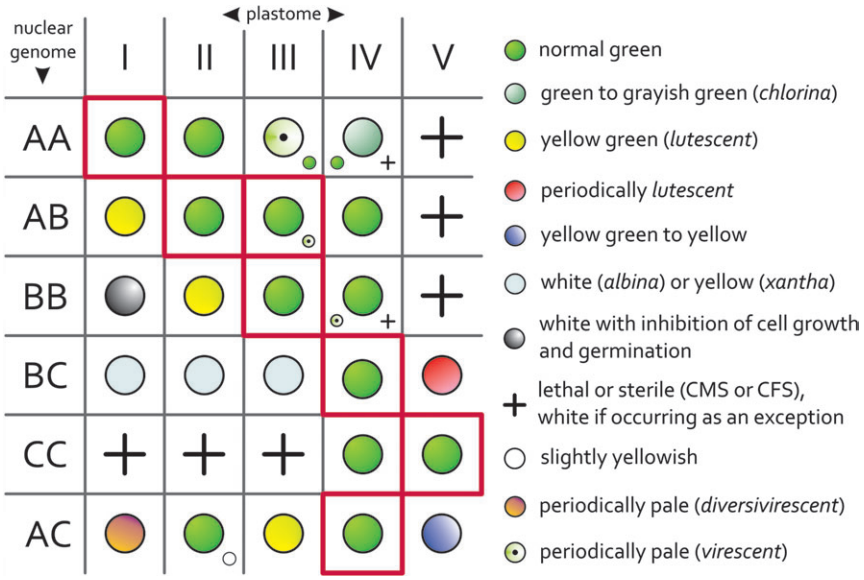

FIG. 2.—Plastome–genome compatibility/incompatibility in the subsection *Oenothera* (redrawn from Stubbe 1989 with permission). A, B and C represent the basic haploid nuclear genomes, I–V the 5 genetically distinguishable plastomes. Genotypes boxed in bold represent naturally occurring species. Minor symbols indicate exceptions noted for some nuclear subgenotypes.

(Mráček et al. 2006), and sequenced representatives of the 5 basic, genetically distinguishable *Oenothera* plastomes (Greiner et al. 2008). The latter paper summarizes the sequence comparison of the 5 chloroplast chromosomes, their phylogenetic relationships, and an idea of the temporal succession of speciation events. The deduced relationships were largely congruent with the plastome pedigree derived from the patterns of plastome–genome incompatibility (PGI) and differences in multiplication rates of plastid types that is a heritable trait associated predominantly with the plastome and subject to selection (reviewed in Chiu et al. [1988]). In this communication, we endeavor a novel approach by combining this sequence information and bioinformatic approaches with formal genetic data to unveil regions on the plastid chromosomes that are potential candidates for plastome-encoded determinants of interspecific PGI. The incompatible combination AB-I was selected as a case study to demonstrate the feasibility of the strategy.

Materials and Methods

Plant Material

The naturally occurring species *Oenothera elata* subsp. *hookeri* strain johansen (^{h}johansen·^{h}johansen I^{joh}; AA-I) (Cleland 1935) and *Oenothera grandiflora* strain tuscaloosa (^{h}tuscaloosa·^{h}tuscaloosa III^{tusc}; BB-III) (Steiner and Stubbe 1984) were used to generate incompatible AB-I and compatible AB-III hybrids. Because plastids are transmitted biparentally in *Oenothera* and segregate somatically in the F1 generation, AB-I and AB-III hybrids, ^{h}johansen·^{h}tuscaloosa I^{joh} and ^{h}johansen·^{h}tuscaloosa III^{tusca}, respectively, can be generated directly from a cross of both species. Compatible and incompatible tissue segregates on the same individual, which is of advantage for comparative analysis of gene expression. Segregation of plastomes was checked by polymerase chain reaction (PCR)–based polymorphisms (plastome I^{joh}, GenBank accession number EU262894, and III^{tusca}, GenBank accession number EU262904). An AB hybrid with another subplastome III (III^{lam}) was selected as a control to confirm plastome III specificity of the genetic pattern. The hybrid containing plastome III of *Oenothera glazioviana* strain rr-lamarckiana Sweden (Heribert-Nilsson 1912) was generated from a cross between *O. elata* subsp. *hookeri* strain johansen equipped with plastome III^{lam} (AA-III^{lam}) and *O. grandiflora* strain tuscaloosa. No notable difference between the 2 green AB-III F1 hybrid lineages (AB-III^{lam} and AB-III^{tusca}) could be detected. Crossings, growth conditions, and phenotypic markers for identification of the hybrids were described previously (Steiner and Stubbe 1984; Dietrich et al. 1997).

Various *Oenothera* species and strains listed in Supplementary table 1 (Supplementary Material online) were investigated to monitor the specificity of the deletion in the *clp*P–*psb*B spacer region for plastome type I variants, that is, from 9 subplastomes I and 2 subplastomes each of plastomes II, III, and IV. The relevant sequence interval was PCR amplified with the primer pair VP9for 5′-catcttcttcgtcttcgtctcc-3′ and VP10rev 5′-aatacacccaatgccagatagc-3′ and sequenced.

Plastome Sequences

Sequences of the 5 basic plastomes of subsection *Oenothera* are deposited in GenBank (accession numbers: AJ271079.3, EU262887, EU262889, EU26890, and EU262891, respectively). Their design and differences in gene-coding and intergenic regions have been discussed previously (Greiner et al. 2008).

Identification of Potential Editing Sites

Differences between deduced protein sequences of *Oenothera* and the corresponding components of *Marchantia polymorpha* (X04465) that lacks RNA editing (Freyer et al. 1997) have been computationally analyzed whether a C-to-U substitution within the respective codon may restore the liverwort sequence. Such positions are designated potential editing sites in *Oenothera* genes.

Analysis of Variable Amino Acid Sites

To estimate the impact of a single amino acid exchange to PGI within *Oenothera*, 2 characteristics were considered. First, mutations exchanging amino acids with highly different biochemical properties have an increased likelihood to alter or destroy protein function. The skewness of biochemical properties at a variable site was therefore estimated within the 5 *Oenothera* plastomes. Second, highly conserved sites are less likely to undergo a drastic change. Hence, a background distribution of the biochemical properties of sites was derived from multiple alignments of sequences from 30 reference species covering dicots as well as monocots.

Biochemical property distributions were generated as follows: Let c be a specific column in the alignment of N species and $C = \{x_i\}, i = 1, 2, \ldots N$, the set of letters x of the ith species at c. Given the Grantham (1974) Matrix as a distance function d, $D := \{d(x_i, x_j) \mid x_i \in C,\ x_j \in C,\ i < j\}$ defines a distribution of pairwise differences of biochemical properties between all species at position c. To enrich for PGI candidate sites, we tested for significant differences ($P \leq 0.05$) by a nonparametric Wilcoxon rank sum test (http://www.r-project.org/index.html) between the distributions derived from sequences of the 5 *Oenothera* and reference species, respectively. Note that the test excludes also sites that represent an *Oenothera*-specific adaptation, that is, sites that are similar within each data set but dissimilar between both sets. The *Oenothera* mutations were also checked whether they are located within known functional regions. Protein domains (e values $\leq 1 \times 10-10$) were detected using the PFAM database (Bateman et al. 2004). Transmembrane domains were located by the InterPRO database (http://www.ebi.ac.uk/interpro) and analyzed with the online DAS server (Cserzo et al. 1997).

Estimation of *K*a/*K*s Substitution Rates

Nonsynonymous and synonymous substitution rates were determined using the yn00 program of the PAML

package (Yang 1997). F3x4 were selected as substitution matrix, and *K*a and *K*s were determined by the Nei–Gojobori method as implemented in yn00. Rates for protein-coding genes variable among at least 2 of the 5 *Oenothera* plastomes were estimated from pairwise codon-based alignments. There are 10 pairwise combinations for each gene, resulting in a total of 780 rates for all and 470 rates for variable genes. Note that the computation of $\omega = Ka/Ks$ is not always applicable (e.g., for $Ks = 0$). Therefore, ω could be determined for only 215 pairwise combinations. Mean ω, *K*a, and *K*s values for a species were obtained from concatenated alignments of single gene alignments. Only orthologous genes present in *Oenothera* and all reference plastomes have been used for this approach.

Photosystem II Quantum Yield and Photosystem I Redox State

Efficiency and functional state of photosystem (PS) II reflected by chlorophyll *a* fluorescence parameters at room temperature (Schreiber et al. 1998) were calculated from wild-type (AA-I and AB-III) and incompatible (AB-I) rosette leaves using a pulse-modulated fluorimeter (PAM 101, Walz, Effeltrich, Germany). The light intensity of the modulated measuring beam (1.6 kHz) was 0.5 μmol $m^{-2}\ s^{-1}$. Leaves, dark adapted for 10 min, were used to detect the intrinsic (Fo) and maximal (Fm) fluorescence yields, the latter being determined by application of a saturating light pulse (0.8 s, 7,000 μmol $m^{-2}\ s^{-1}$). The potential maximum quantum yield was calculated as $(Fm - Fo)/Fm = Fv/Fm$. Red actinic light (650 nm, 50 μmol $m^{-2}\ s^{-1}$) was used for measurements of fluorescence quenching. Nonphotochemical quenching (NPQ) was determined by applying repetitive saturation pulses with 20-s intervals and calculated as $(Fm' - F)/(Fm' - Fo)$ (Kooten and Snel 1990).

The light-dependent redox state of PSI was measured on leaves as absorption changes at 830 nm in the absence or presence of actinic (650 nm, 50 μE $m^{-2}\ s^{-1}$) and far-red light (12 Wm^{-2}) using the PSI attachment of PAM101 (Klughammer and Schreiber 1998). Saturating light pulses (0.8 s, 7,000 μmol $m^{-2}\ s^{-1}$) were applied to follow PSII-dependent reduction of PSI in far-red background light.

Results

General Features

The geographical distribution and genomic constitution of the 11 genuine species of the North American subsection *Oenothera*, with their basic genomes A, B, and C associated with their respective plastomes I–V are illustrated in figure 1. In a preceding publication, we presented the complete nucleotide sequences of representatives of the 5 basic *Oenothera* plastomes, their comparison, evolutionary relationships, and temporal relation (Greiner et al. 2008). All 5 genomes are perfectly colinear and deletions, rearrangements as well as duplications of entire genes were not detected. Such sequences from closely related, morphologically distinct, and still interbreeding species for which an organelle and nuclear genetics including cybrid technology is available for the first time offered the possibility to search for genetic determinants causal to compartmental coevolution. Numbers of single mutations like small indels or replacements of nucleotides are in the range of several thousands if each pairwise plastome comparison is considered. To delineate candidate PGI determinants, we analyzed single- or small-scale molecular differences between orthologous genetic elements, notably coding sequences and predicted functional elements in intergenic regions. Four computational approaches were employed to delimit candidate sequences for PGI: 1) estimation of evolutionary rates for protein-coding regions, 2) analysis of predicted or known polypeptide variance, 3) RNA editing patterns, and 4) phylogenetic footprinting of polymerase binding sites. This evolutionary sequence filtering approach was based on a comparison of sequence differences with the incompatibility chart of subsection *Oenothera* listing all possible genome–plastome combinations, which are either compatible or incompatible (fig. 2). For instance, genetic polymorphisms could be excluded to be causative for incompatibility when any other plastome containing polymorphic sequences identical to the incompatible plastome was compatible in the respective nuclear background. On the other hand, polymorphisms in genes, which could not explain an incompatible phenotype, were excluded from the list of potential candidates for PGI. As a case study, the bioinformatics and formal genetic data were complemented by biophysical measurements of the incompatible AB-I combination.

Estimation of Selection Pressure on *Oenothera* Plastomes

Genes causative for speciation have been suggested to be under positive selection for a limited period. Positive selection on plastid genes has not been reported, except recently for *clp*P and *rbc*L in *Oenothera* and other taxa (Kapralov and Filatov 2007; Erixon and Oxelman 2008). To estimate selection pressure on the *Oenothera* plastomes and to derive candidate genes for incompatibility factors, ratios of nonsynonymous (*K*a) versus synonymous (*K*s) substitutions were determined for genes, varying within the 5 plastomes, using alignments of their entire coding sequences. Out of 233 pairwise comparisons for which the method was applicable, 33 (14.1%) exhibited elevated *K*a/*K*s rates above 1.0. Notably, an excess of nonsynonymous substitutions was not equally distributed between the pairs under study but clustered predominantly to 5 genes, *ycf*1, *ycf*2, *acc*D, *clp*P, and *ndh*A (Supplementary table 2, Supplementary Material online). For almost all plastome pairs, these genes displayed ω values greater than 1, which indicates positive selection. The first 3 genes contain extended repetitive regions that are only weakly conserved in other species. It is therefore unclear whether divergence of these regions is functionally relevant or whether the increase of nonsynonymous substitution rates is simply the result of observed high variability. The highest rates ($\omega = 4.1$) calculated for *clp*P seem to differentiate plastomes I and II versus III, whereas maximal rates for *acc*D ($2.2 < \omega < 4$) were observed between clade I/II and IV and V, respectively. A similar, though less

Table 1
Average *Ka*/*Ks* Values Calculated from the 5 *Oenothera* Plastomes in Pairwise Comparison

Ka/*Ks* (*Ka*; *Ks*)	Plastome I	Plastome II	Plastome III	Plastome IV
Plastome II	0.6266 (0.0002; 0.0003)	—	—	—
Plastome III	0.5107 (0.0009; 0.0017)	0.5945 (0.0009; 0.0015)	—	—
Plastome IV	0.4176 (0.0013; 0.0030)	0.4567 (0.0013; 0.0029)	0.4446 (0.0013; 0.0030)	—
Plastome V	0.4608 (0.0017; 0.0036)	0.4961 (0.0018; 0.0036)	0.4309 (0.0015; 0.0034)	0.2371 (0.0006; 0.0025)

pronounced, observation has been made for *ndh*A. Together, elevated rates in the 5 genes comprise 26 of 33 pairs with positive selection. For *ccs*A, *pet*D, and *mat*K each, only one pairwise ω value exceeded the chosen criterion for positive selection. However, we note that several pairs of *mat*K and *ccs*A indicate elevated evolutionary rates well above the median $\omega = 0.405$. Clustering of elevated rates has also been observed for *ndh*D, *rps*18, and *rps*3 (Supplementary table 2, Supplementary Material online). The mean *Ka*/*Ks* ratio $\omega = 0.166$ for pairwise comparisons of 30 angiosperm chloroplast genomes showed only a small variance (standard deviation: 0.03) in most branches of the mono- and eudicotyledonous plants investigated. Most ratios between *Oenothera* plastomes, however, were considerably higher (mean *Ka*/*Ks* ration $\omega = 0{,}47 \pm 0.11$, Student's *t*-test: $P < 10^{-6}$), with a minimum of 0.24 between plastomes IV and V and a maximum of 0.63 for plastomes I and II (table 1). The unusually high mean *Ka*/*Ks* ratios between most of the 5 plastomes and the relatively large number of genes indicating positive selection or fast evolutionary rates are consistent with a significant contribution of plastomes to speciation.

Search for Candidate Protein-Coding Loci Involved in PGI

Two attempts were made to estimate the impact of plastome-specific differences in genes. First, a putative functional impact of nonsynonymous sites in polypeptides was estimated from the degree of conservation and differences of biochemical properties between *Oenothera* and 30 reference species as described in Materials and Methods. Starting from 388 nonsynonymous replacements, excluding *ycf*1, *ycf*2, and the highly variable *acc*D N-terminus (Greiner et al. 2008), 35 sites in 19 polypeptides were identified that showed a significant difference between the distribution of biochemical properties within *Oenothera* and to reference species ($P < 0.05$). Twenty-five of the significant sites were located within a known PFAM domain (Supplementary table 3, Supplementary Material online). Note that almost all genes with elevated *Ka*/*Ks* rates are present in the set of 19 proteins.

Second, protein-coding genes with length polymorphisms are of intrinsic interest for PGI. Relevant are 2 genes, *atp*A and *psb*B, from which the electrophoretic mobility is known to differ in plastomes III, IV, and V, respectively (Herrmann and Possingham 1980), and 8 loci that predictably should generate variant polypeptides between the evening primrose plastomes (Greiner et al. 2008). The latter was arbitrarily divided into 2 groups, those with (*ndh*D, *rpl*22, and *rps*18) and those without reading frameshifts (*ycf*1, *ycf*2, *acc*D, *clp*P, and *ndh*F). Pairwise as well as multiple protein alignments between these primrose size variants and their orthologs in 4–8 reference plastomes were manually edited and compared with the plastome–genome compatibility scheme of subsection *Oenothera* (fig. 2). Briefly, alternative stop codons caused by single-base pair indels were found for *ndh*D (plastome I) and *rpl*22, multiple base pair indels leading to different stop codons for *acc*D, *clp*P, *ndh*D (plastome V), *ndh*F, and *rps*18; a point mutation causes a change of the stop codon in *atp*A of plastome III, and a single G (IV, V) to A (I, II, III) conversion at position 1195 in *psb*B leads to a conservative change from valine to isoleucine (Supplementary table 5, Supplementary Material online). The *ycf*1 and *ycf*2 genes are only moderately conserved in plastid genomes in general, and AccD is highly polymorphic in its N-terminal region as in the reference plastomes. Length polymorphisms in *acc*D, *atp*A, *clp*P, *ndh*D, *ndh*F, *rpl*22, and *rps*18 could not be compared with distinct amino acid residues. However, none of these regions, except the altered *ndh*D 3′ terminus, is located within a functional domain (Supplementary table 5, Supplementary Material online). Computational analysis of transmembrane domains was used also to check each candidate for aberrations in its transmembrane domain architecture. Marginal effects appeared only for components of the NAD(P)H dehydrogenase complex, for *ndh*A, *ndh*D, and *ndh*E (data not shown). Apart from the fact that it is unclear whether the predicted relatively small perturbations alter notably the stability of the transmembrane regions, disruption of *ndh* genes in tobacco did not result in a pronounced phenotype (Burrows et al. 1998; Kofer et al. 1998). Details of the changes in these loci including verification by PCR analysis as well as comparison with loci of reference species and their interpretation are therefore presented in Greiner et al. (2008; supplementary figs. S1–S5, Supplementary Material online).

Supplementary tables 3 and 5 (Supplementary Material online) list the possible role of each of the significant mutations in coding regions for both single amino acid exchanges and variant polypeptides caused by indels for the distinct plastome–genome combinations in the compatibility scheme (fig. 2).

Role of RNA Editing in PGI

The findings that editotypes in plastids may differ between related species and even between ecotypes (Tsudzuki et al. 2001; Tillich et al. 2005) and that plant-specific editing sites often cannot be modified heterologously (Schmitz-Linneweber et al. 2005; Shikanai 2006) have been suggested that this kind of RNA maturation plays a crucial role

not only in translation but also in speciation processes (Schmitz-Linneweber et al. 2001, 2005). Editing of the *ndh*D ACG start codon in plastomes I and IV as in spinach, tobacco, and *Antirrhinum* (Neckermann et al. 1994) established the presence of an editing system in evening primroses. Comparison of the protein-coding sequences with those of the liverwort *M. polymorpha*, which lacks RNA editing uncovered 320 potential sites in coding regions in *Oenothera* (data not shown). These sites represent a comprehensive capture of all possible editing sites including true sites (in higher plants usually in the order of 30–35) and a large fraction of false positives. Despite this high number, only a single-nucleotide substitution differs among the potentially edited sites in the Onagracean plastomes. *Ndh*A of plastomes I, II, and III contains a C-to-T conversion at amino acid position 309 compared with plastomes IV and V which would result in a T-to-I amino acid change. Because knockout lines of genes for nicotinamide adenine dinucleotide phosphate dehydrogenase (NDH) subunits in tobacco display no or only subtle phenotypes (Burrows et al. 1998; Kofer et al. 1998), editing—in contrast to the Solanacean model (Schmitz-Linneweber et al. 2001, 2005)—does not play a crucial role in speciation of the *Oenothera* clade nor in the generation of interspecific plastid–nuclear incompatibility.

Search for Candidate Loci for PGI in Intergenic Regions

The differences located in promoter sequences of the *Oenothera* plastomes were compared with the genetically determined compatibility relationships in interspecific hybrids (fig. 2) in order to classify them and to pinpoint potential determinants contributing to PGI.

Two types of RNA polymerases operate in plastids of higher plants, the ancient eubacterial type polymerase (PEP) and an acquired phage-type polymerase (NEP) (Shiina et al. 2005; Liere and Börner 2006). The polymerases recognize distinct sites in plastid promoters. In all, 38 putative PEP- and 25 NEP-binding sites that were computationally predicted were altered in at least one of the plastomes (Greiner et al. 2008). Mutations were classified according to 3 criteria: 1) their similarity to an ideal consensus (Silhavy and Maliga 1998; Kapoor and Sugiura 1999; Homann and Link 2003; Kanamaru and Tanaka 2004; Shiina et al. 2005; Liere and Börner 2006), 2) number, and 3) position of predicted polymerase binding sites relative to a translational start site (supplementary table 4A and B, Supplementary Material online). With this selection scheme, 9 putative PEP promoters, notably of *clp*P, *psb*B, *rpl*16, *rpl*33, *rps*12, *rps*15, *trn*G_{GCC}, *trn*L_{CAA}, *trn*S_{UGA}, and 7 predicted NEP promoters, namely of *atp*H, *clp*P, *ndh*G, *psb*B, *psb*K, *rps*4, and *trn*G_{GCC}, were deduced as candidates causing PGI. Three promoter sequences indicated drastic changes for both polymerases: the promoter of *trn*G_{GCC} harboring mutations specific for plastome V, and the bidirectional promoters for *clp*P (encoding a catalytic subunit of the protease Clp) and *psb*B (encoding the chlorophyll *a*–binding protein CP47 of the PSII core complex) that contain a large deletion specific for plastome I.

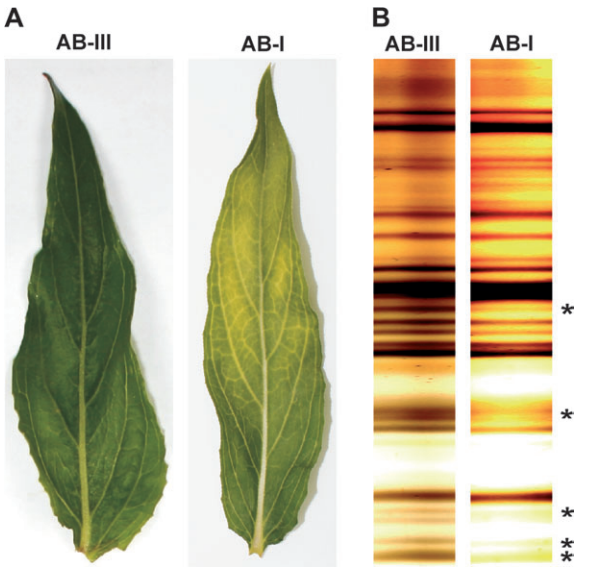

FIG. 3.—(*A*) Phenotype of compatible AB-III control and incompatible, *lutescent* AB-I hybrid leaves. (*B*) Silver-stained thylakoid membrane proteins of AB-III and AB-I hybrids showing a comparable protein pattern and only deficiencies of some specific, presumably PSII, proteins in AB-I, which are labeled by asterisks.

Delineation of an AB-I Incompatibility Determinant: The *clp*P–*psb*B Intergenic Region

Variant sequence regions in plastomes I–V were systematically compared with compatibility/incompatibility patterns (fig. 2) to filter loci relevant for PGI. This approach finally correlated the AB-I phenotype with a single major locus, the intergenic region *psb*B–*clp*P. AB-I displays a yellow–green (*lutescent*) phenotype (fig. 3*A*). The plastome–genome combinations AB-II and AB-III, which both occur in nature, and the hybrid containing plastome IV are green (fig. 2; Stubbe 1989). In this distinct case, changes in plastome I shared with or similar to at least one in plastomes II–IV can be disregarded. Plastome V was excluded from our analysis because the combinations AB-V, AA-V, and BB-V are extremely disharmonic and differ substantially from the AB-I phenotype. They are fully bleached, largely pollen sterile, and display severe inhibition of cell division (Stubbe 1963). The principal genetic determinants responsible for their phenotypes are presumably complex and different from those causing bleaching of AB-I individuals (see Discussion).

The outlined filtering strategy uncovered 22 regions, including minor changes such as single nucleic acid exchanges in noncoding regions. Six of them are polymorphic within all plastomes. A contribution of these regions to PGI is unlikely because plastomes II, III, and IV remain fully compatible in an AB background (fig. 2). This excludes the genes *acc*D, *ycf*1, and *ycf*2, the intergenic regions *rps*16/*rbc*L and *trn*Q_{UUG}/*acc*D, as well as the SSC/IR_A junction. Sixteen regions specifically altered in plastome I remain. All regions involving the NADPH complex can be disregarded because knockouts of individual NDH subunits in tobacco lack a conspicuous phenotype (Burrows et al. 1998; Kofer et al. 1998). Therefore, the length variance of NdhD and NdhF (supplementary table 5, Supplementary Material online) as well as of the

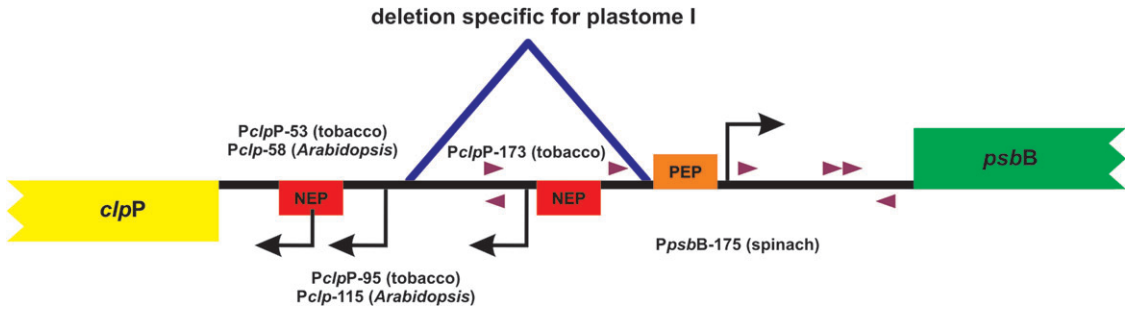

FIG. 4.—Schematic overview of the *clp*P/*psb*B spacer region in *Oenothera*, spinach, tobacco, *Atropa*, *Eucalyptus*, *Gossypium*, and *Arabidopsis*. Positions of the indicated transcription start sites (black arrows) of NEP and PEP promoters (P*clp*P and P*psb*B) relative to the start codons were determined experimentally in *Arabidopsis*, tobacco, and spinach (Westhoff 1985; Hajdukiewicz et al. 1997; Sriraman et al. 1998; Swiatecka-Hagenbruch et al. 2007). Putative, not experimental verified promoters in *Oenothera* are marked with filled triangles. The experimentally verified P*clp*P-173 and P*psb*B-175 are highly conserved and confirmed bioinformatically in *Oenothera* and all references species. The deletion (open triangle) is not present in *Oenothera* plastomes II–V or plastomes of other species sequenced so far and, therefore, specific for plastome I in *Oenothera*.

intergenic regions *ndh*G/*ndh*I, *ndh*I/*ndh*H, *ndh*F/*rpl*23, or *ndh*F/*trn*N_{GUU} can be excluded. Additional noncoding regions, such as the *atp*I/*atp*H spacer and a small deletion downstream of the *pet*N stop codon, are not involved in the AB-I phenotype because neither the ATP synthase nor of the cytochrome complex are affected in AB-I tissue as revealed by immunological analysis (data not shown). Specific variations left are small deletions in the intron of *rpl*16, the 5′ region of *rpl*32, the *trn*G_{UCC}/*trn*S_{GCU}, *trn*L_{UAA}/*trn*T_{UGU}, and *rps*8/*rpl*14 spacers, and a single amino acid exchange in Rpl32. They are not of functional relevance because the translational apparatus is not notably affected in AB-I as could be judged by silver staining of thylakoid membrane proteins (fig. 3*B*). Therefore, only 2 regions remain, which serve as putative candidates. First, a small deletion in the promoter of *psb*I in the intergenic spacer of *psb*I and *psb*K, and second, a large deletion in the *clp*P/*psb*B spacer, affecting both NEP and PEP promoters (fig. 4; supplementary table 4A and B, Supplementary Material online). The involvement of the *psb*I promoter in the AB-I phenotype is rather unlike because 1) mRNA levels of *psb*I are not changed (data not shown) and 2) a knockout of *psb*I shows no apparent phenotype (Schwenkert et al. 2006). Consequently, only the 148-bp deletion at position 77,080 of plastome I^{joh} (GenBank accession number AJ271079.3) in the intergenic *clp*P/*psb*B region remained as the only potential plastid component responsible of the AB-I incompatibility. Three approaches were employed to substantiate this deduction.

First, sequence analysis of intraplastome variance (Herrmann et al. 1980) of the *clp*P–*psb*B spacer region corroborated that the deletion is plastome I-specific. It was present in 9 different plastome I subtypes found in 3 species or subspecies (GenBank accession numbers: EU449954–EU449961 and AJ271079.3) but not in the 6 variants investigated for plastomes II, III, and IV (GenBank accession numbers: EU262889, EU262890, EU262891, EU449963, EU449962, and EU449964) that were derived from 5 different species. Furthermore, all these subplastomes were checked genetically, and only plastome I variants were found to cause incompatibility with genotype AB (see references in supplementary table 1, Supplementary Material online).

Second, a phylogenetic footprinting analysis of the intergenic region between both genes delimited distinct boxes in the promoter region described for *clp*P (Sriraman et al. 1998) and *psb*B (Westhoff 1985; Westhoff and Herrmann 1988) and uncovered substantial changes to *Oenothera* and among its plastomes. Notably, a large deletion in plastome I directly upstream of the highly conserved *psb*B PEP promoter and the *clp*P 5′ region eliminated a putative and a confirmed *clp*P promoter and 2 putative *psb*B promoters (data not shown) (fig. 4). Conservation as well as similarity to known sites in other species suggested that an element missing in plastome I caused the specific adaptation of plastome I to the AA genome and that the change of this region leads to an altered expression of *psb*B and/or *clp*P in the AB-I combination.

Third, if altered expression of *psb*B and/or *clp*P contributes to the bleaching of the AB-I phenotype, decreased PSII activity/levels and eventually pleiotropic effects due to *clp*P overexpression would be expected. Thus, the activity of PSII relative to that of PSI was monitored by spectroscopic analyses (fig. 5). Chlorophyll fluorescence induction was measured on dark-adapted leaves to adjust an oxidized plastoquinone pool of incompatible AB-I and compatible AB-III and AA-I plants. Maximum PSII quantum efficiency (Fv/Fm) was in fact reduced to 0.52 ± 0.04 in the incompatible AB-I leaf compared with 0.79 ± 0.03 in AB-III or AA-I consistent with a deficiency in PSII activity. The low Fv/Fm ratio observed was caused by an elevated Fo and decreased Fv fluorescence level in AB-I indicating inefficient exciton transfer to the reaction center and/or malfunction of PSII (fig. 5). The fluorescence level elicited by moderate actinic light (50 μE m^{-2} s^{-1}) dropped far below the initial Fo level depending on the light intensity indicative defects in photosynthetic light utilization. Actinic light-induced quenching of chlorophyll fluorescence was faster in AB-I than in AB-III or AA-I, and a longer period was required to reach the steady state. NPQ increased dramatically from 0.39 ± 0.14 in AA-I and AB-III to 2.47 ± 0.42 in AB-I indicating an imbalance of photosynthetic electron transport. After switching off actinic light, the fluorescence decayed to the former Fo level in AA-I and AB-III but increased in AB-I within several minutes to finally reach the increased Fo already observed during

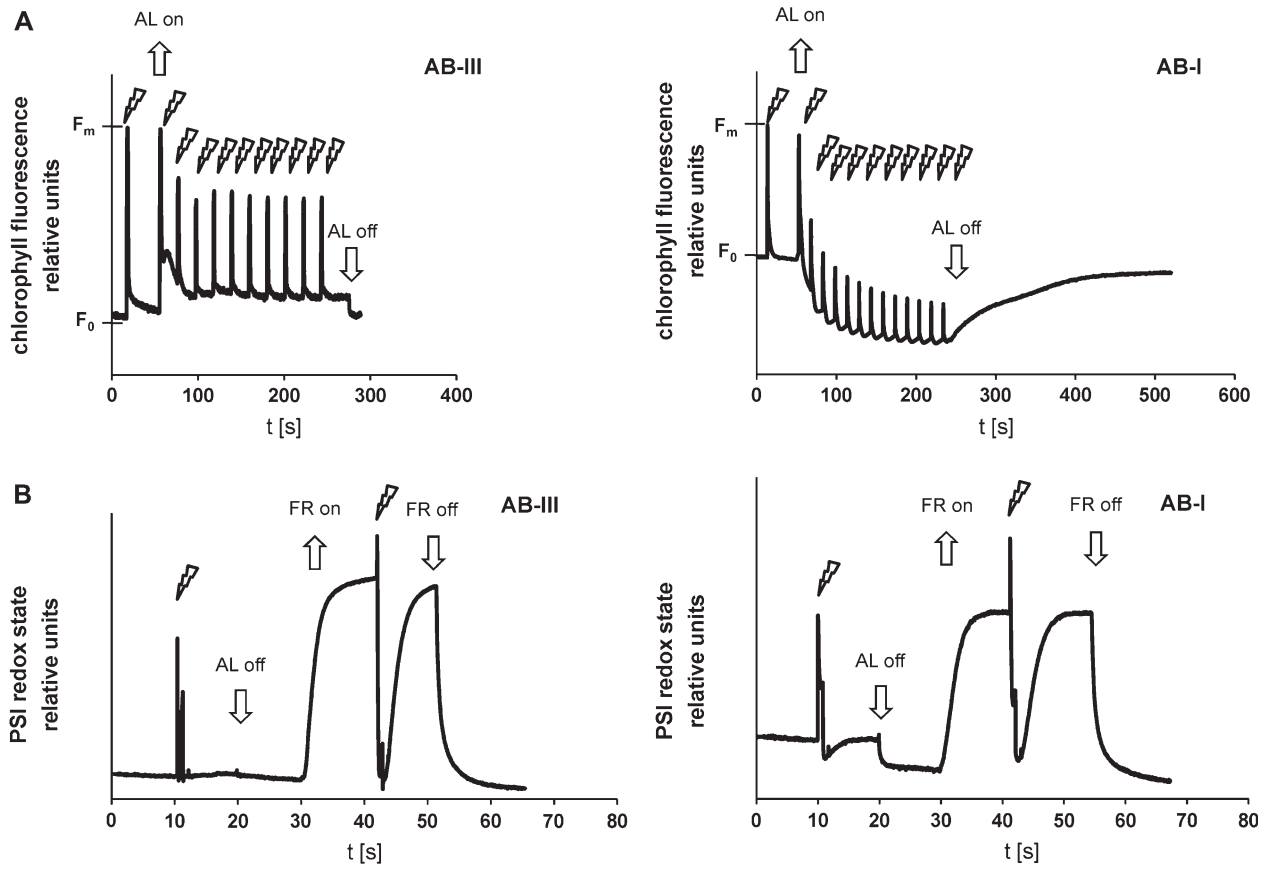

FIG. 5.—Studies on photosystem II yield and redox kinetics of photosystem I. (*A*) Fluorescence induction kinetics of compatible AB-III and incompatible AB-I leaves. Fluorescence induction traces induced by saturating white-light pulses showed the maximal fluorescence raise during the light pulse (Fm). The Fm levels were normalized to equal heights. Dark-adapted leaves were exposed to consecutive saturating light pulses during application of continuous actinic light. (*B*) The P700 oxidized state of compatible and incompatible leaves exposed to 50 μE m^{-2} s^{-1} actinic red light was recorded. The signal level of AB-III was not affected after switching off the actinic light (downward black arrow) indicating that PSI is largely reduced. However, significant absorbance changes were recorded after switching off actinic light in AB-I indicating that a substantial part of PSI was oxidized due to deficiencies of PSII. Application of FR light (upward open arrow) oxidized PSI in both compatible and incompatible leaves. Subsequent saturating light pulses (squiggled arrows) on the FR background light transiently reduced PSI completely in compatible but only partially in incompatible leaves again indicating a limitation of PSII activity. AA-I plants resembled in their PSII fluorescence and PSI redox characteristics those of AB-III (data not shown).

the dark adaptation prior to the measurement, again indicating malfunction of PSII. Application of far-red light, which preferentially excites PSI had no notable effect on the half-life of the fluorescence rise upon light/dark switches nor on the elevated Fo levels suggesting that the AB-I incompatibility reflects a direct effect on PSII-driven electron transport, such as stable accumulation of Q_A species in the dark which induces an increased Fo level.

The extent of PSI oxidation in terms of balanced electron flow from PSII to PSI was monitored using absorption changes at 830 nm on actinic background light in order to further substantiate the primary lesion in the hybrid (fig. 4). Although PSI signal intensity in AB-I was generally slightly reduced, the results clearly showed a much higher actinic light-induced oxidation state of PSI in AB-I compared with AB-III. At 50 μE m^{-2} s^{-1}, about 15% of P700 was oxidized in AB-I, whereas the reaction center of PSI remained almost completely reduced in AB-III, a response likely due to limited electron flow toward PSI of a deficient PSII rather than of downstream effects in the AB-I hybrid. Furthermore, short light pulses at far-red background light were sufficient to completely reduce PSI in AB-III and AA-I but not in AB-I, indicating a slower PSII-mediated electron transport. Taken together, chlorophyll fluorescence analysis is fully consistent with a decreased PSII activity relative to PSI and suggests that the lesions in the incompatible AB-I hybrid primarily affect PSII function. A detailed molecular analysis of the incompatible AB-1 phenotype will be presented in a forthcoming study.

All data obtained not shown in the manuscript are available upon request.

Discussion

Compartmental coevolution is accompanied by distinct changes in the 5 available Onagracean organelle chromosomes and the respective nuclear genomes. In subsection *Oenothera*, relationships between plastome and genome are crucial for the vitality of interspecific hybrids (Stubbe 1964; Dietrich et al. 1997). All its species can

be crossed with one another, forming seeds with fully developed hybrid embryos that usually germinate and produce fertile progeny. However, the development of such hybrids is frequently disturbed and limited only by incompatibilities between the plastome of one parent plant with the genotype of the other one when the genetic compartments were not coevolved (fig. 2). Reversibility of interspecific compartmental incompatibility is a distinguishing feature to nuclear and plastid mutations affecting the organelle; an incompatible plastid foreign to a nucleus, for instance, will regreen if recombined with its genuine genome. Therefore, PGI is not based on mutations in single genes but in changed interactions of coevolved gene pairs, one of which resides in the chloroplast, the other in the nuclear genome. These PGI gene pairs represent a special case of the Dobzhansky–Muller model underlying their impact in speciation processes (Dobzhansky 1937).

Disturbances caused by interspecific organelle exchanges normally affect a multitude of ontogenetic processes. Most conspicuously are lesions of the photosynthetic machinery (hybrid bleaching, hybrid variegation) and of the generative phase that can be impaired at various gametophytic and/or sporophytic stages, such as pollen and/or ovule development (summarized in Harte [1994]). Both, photosynthetic performance and hybrid fertility are complex characters with a large number of potential states. Thus, PGI phenotypes are probably caused by processes that operate at many scales. This intricacy is not unexpected because about 30% of the nuclear coding capacity is required for the management of the organelles (Herrmann 1997). Complexity also becomes apparent in various extremely disharmonic plastome–genome incompatible hybrids such as AA-V, AB-V, and BB-V, in which fertility and morphogenesis are severely affected (Stubbe 1963; Stubbe et al. 1978). In these cases, incompatibility may be caused by multiple Dobzhansky–Muller plastid–nuclear gene pairs. The profound knowledge of the photosynthetic process and of the biogenesis, maintenance, and adaptation of its underlying structures (Herrmann and Westhoff 2001) can advantageously be used for evaluating phylogenetic questions and provide general and causal access to evolutionary relationships and speciation processes.

The relatively large number of plastome-encoded genes deduced to be under positive selection or displaying fast evolutionary rates, manifesting in high *K*a/*K*s values, clearly reflect an active contribution of plastomes to speciation. However, our knowledge to computationally predictable functional elements from primary sequences is limited, and *Oenothera* genome sequences—the complementary part on which prespeciation and coevolution processes are acting—are missing. Nevertheless, the alignment of sequence differences between plastomes of closely related, interbreeding species to predict genetic elements combined with filtering by their evolutionary and functional relevance as well as combinatorial logics is a promising strategy to pinpoint potential plastid-localized determinants involved in compartmental coevolution last not least because predictions can be tested. The case study of the hybrid AB-I has proven that the strategy of systematic filtering on genetically well-defined material is useful and attests to the power of the method. It correlated the bleached AB-I phenotype with a distinct major locus, a plastome I–specific deletion in the *clp*P–*psb*B intergenic region with reduced PSII activity in AB-I. Bioinformatic and biophysical data are consistent with a primary lesion in PSII and reminiscent to PSII downregulation in a bleached *Arabidopsis* mutant with severe deficiencies of *psb*B transcripts and CP47 proteins (Meurer et al. 1996, 2002). This mutant also displays comparable fluorescence characteristics. Loci such as the *clp*P–*psb*B intergenic region deduced by this approach are therefore potential candidates that deserve further study of underlying molecular mechanisms of PGI.

At a molecular scale, coevolution of polypeptides with their interaction partners, polypeptides with polypeptides or polypeptides with nucleic acid molecules, is a well-known phenomenon (Goh et al. 2000). Basically, it could reflect a regulatory and/or a structural phenomenon. Diverging loci (supplementary table 5, Supplementary Material online) are therefore of intrinsic interest but the vast majority of such loci found in *Oenothera* either does not seem to be involved in interspecific compartmental incompatibility or does not contribute in a simple way. All changes occurred in parts of polypeptide chains, which are generally highly variable and do not affect conserved domains (supplementary figs. S1–S5 [Supplementary Material online] in Greiner et al. [2008]). In terms of single amino acid exchanges of all 388 detected nonsynonymous substitutions, only 35 sites from which 25 are located in functional domains show biochemically significant different properties with respect to reference plastomes (supplementary table 3, Supplementary Material online). These sites are encoded by altogether 19 genes, namely *acc*D, *atp*A, *atp*B, *atp*F, *ccs*A, *clp*P, *mat*K, *ndh*A, *ndh*B, *ndh*C, *ndh*D, *ndh*E, *ndh*H, *pet*B, *rpo*B, *rpo*C2, *rps*3, *rps*8, and *rps*15. Current knowledge decreases this small number of candidates even further. For instance, variance of RpoB between tobacco and *Atropa*, initially a candidate for PGI (Herrmann et al. 2003), did not turn out to have a notable influence (Schmitz-Linneweber et al. 2005), or gene deletions in tobacco suggest that disruption of genes for subunits of the NDH complex (Burrows et al. 1998; Kofer et al. 1998) are not of relevance either. Furthermore, a biochemically possibly significant amino acid change in *pet*D fits with the compatibility chart in principle (fig. 2) but appears to be neutral because BB-II does not show a cytochrome phenotype (data not shown). Collectively, the available data strongly suggest that plastome-encoded genes for structural components of the photosynthetic machinery are usually highly conserved. Therefore, we suggest that compartmental coevolution in *Oenothera* influences predominantly gene expression and/or the transcript metabolism, as found also in the Solanacean model (Schmitz-Linneweber et al. 2001, 2005).

Species-specific editotype differences in plastid DNA and coevolving nuclear encoded *trans* factors have been shown to be important in compartmental coevolution between *Atropa* and tobacco. They play a crucial role in harmonious nucleo–plastid interaction between both species and also explain the pronounced phenotypic difference of their reciprocal cybrids (Schmitz-Linneweber et al. 2001, 2002, 2005). RNA editing obviously does not influence compartmental coevolution in evening primroses. Thus,

other aspects must cause or be involved in compartmental divergence, such as transcription and/or transcript stability of photosynthetic genes via interaction with *trans* factors of nuclear origin and corresponding *cis* elements in the *psb*B promoter or of stabilizing elements in 5′ untranslated regions of its mRNA species in the AB-I hybrid. Collectively, these findings suggest that despite of photosynthetic defects in both, *Solanaceae* and *Oenothera*, the determinants and mechanisms causing plastid–nuclear incompatability are quite different. Obviously, the ways in which individual species or genera have evolved, their histories, and adaptation to their present-day habitats are diverse and include changes at quite different molecular levels.

Plastid chromosomes have well-defined structures, a limited coding potential and a conserved design. Their sequences have become a powerful research tool not only to probe into chloroplast biogenesis, function, and engineering but also into eukaryotic genome evolution. Classical data sets such as available for subsection *Oenothera* are of obvious value to study microevolutionary processes. The other subsections of the genus have not yet received a comparably intense genetic study, but quite substantial information is available regarding interfertility and plastid–nuclear compatibility relationships (Stubbe and Raven 1979). As in subsection *Oenothera*, offspring of interspecific crosses within subsections *Raimannia*, *Munzia*, *Nutantigemma*, and *Emersonia* is generally fertile, and even the generation of intersubsectional hybrids is possible, but these are often extremely disharmonic and their fertility is usually reduced (Stubbe and Raven 1979). Evening primroses represent an instructive, unique model because they offer ready, general, and causal access to study processes of microevolution not only for plastome/genome relationships but also of chromosomal evolution, pollination biology, and biogeographical radiation of this subsection in a continental dimension. With the substantial base of knowledge including taxonomic, biogeographical, genetic, and phylogenetic framework, nuclear and organelle genetics, and the current availability of molecular and cell biological strategies of analysis, *Oenothera* provides unique opportunities to overcome limitations of traditional phylogenetic analyses based on mere sequence data and to develop a "functional molecular phylogeny."

Supplementary Material

Supplementary tables 1–5 and figures S1–S5 are available at *Molecular Biology and Evolution* online (http://www.mbe.oxfordjournals.org/).

Acknowledgments

We thank Martina Silber for critical comments, Dario Leister for kindly reading the manuscript, and the Springer-Verlag for permission to adapt figure 2. The project was supported by the Deutsche Forschungsgemeinschaft (SFB-TR1) to R.G.H. and J.M. and the Hanns-Seidel-Stiftung of grants of the Bundesministerium für Bildung und Forschung to S.G. We dedicate this manuscript to the memory of Prof. Dr Rainer M. Maier.

Literature Cited

Bateman A, Coin L, Durbin R, et al. (13 co-authors). 2004. The Pfam protein families database. Nucleic Acids Res. 32:D138–D141.

Burrows PA, Sazanov LA, Svab Z, Maliga P, Nixon PJ. 1998. Identification of a functional respiratory complex in chloroplasts through analysis of tobacco mutants containing disrupted plastid *ndh* genes. EMBO J. 17:868–876.

Chiu W-L, Stubbe W, Sears BB. 1988. Plastid inheritance in *Oenothera*: organelle genome modifies the extent of biparental plastid transmission. Curr Genet. 13:181–189.

Cleland RE. 1935. Cyto-taxonomic studies on certain Oenotheras from California. Proc Am Philos Soc. 75:339–429.

Cleland RE. 1972. *Oenothera* cytogenetics and evolution. In: Sutcliffe JF, Mahlberg P, editors. Experimental botany. London: Academic Press. p. 43–299.

Cserzo M, Wallin E, Simon I, von Heijne G, Elofsson A. 1997. Prediction of transmembrane alpha-helices in prokaryotic membrane proteins: the dense alignment surface method. Protein Eng. 10:673–676.

Dietrich W, Wagner WL, Raven PH. 1997. Systematics of *Oenothera* section *Oenothera* subsection *Oenothera (Onagraceae)*. In: Anderson C, editor. Systematic botany monographs. Laramie (WY): The American Society of Plant Taxonomists. p. 1–123.

Dobzhansky T. 1937. Genetics and the origin of species. New York: Columbia University Press.

Erixon P, Oxelman B. 2008. Whole-gene positive selection, elevated synonymous substitution rates, duplication, and indel evolution of the chloroplast *clp*P1 gene. PLoS ONE. 3:e1386.

Freyer R, Kiefer-Meyer MC, Kossel H. 1997. Occurrence of plastid RNA editing in all major lineages of land plants. Proc Natl Acad Sci USA. 94:6285–6290.

Goh CS, Bogan AA, Joachimiak M, Walther D, Cohen FE. 2000. Co-evolution of proteins with their interaction partners. J Mol Biol. 299:283–293.

Grantham R. 1974. Amino acid difference formula to help explain protein evolution. Science. 185:862–864.

Greiner S, Wang X, Rauwolf U, Silber MV, Mayer K, Meurer J, Haberer G, Herrmann RG. Forthcoming. 2008. The complete nucleotide sequences of the five genetically distinct plastid genomes of *Oenothera*, subsection *Oenothera*: i. Sequence evaluation and plastome evolution. Nucleic Acids Res. 36:2366–2378.

Hajdukiewicz PT, Allison LA, Maliga P. 1997. The two RNA polymerases encoded by the nuclear and the plastid compartments transcribe distinct groups of genes in tobacco plastids. EMBO J. 16:4041–4048.

Harte C. 1994. *Oenothera*: contributions of a plant to biology. In: Frankel R, Grossman M, Linskens HF, Maliga P, Riley R, editors. Monographs on theoretical and applied genetics. Berlin (Germany): Springer. p. 1–261.

Heribert-Nilsson N. 1912. Die Variabilität der *Oenothera Lamarckiana* und das Problem der Mutation. Z indukt Abstamm Vererbungsl. 9:89–231.

Herrmann RG. 1997. Eukaryotism, towards a new interpretation. In: Schenk HEA, Herrmann RG, Jeon KW, Müller NE, Schwemmler W, editors. Eukaryotism and symbiosis. Berlin (Germany): Springer. p. 73–118.

Herrmann RG, Maier RM, Schmitz-Linneweber C. 2003. Eukaryotic genome evolution: rearrangement and coevolution of compartmentalized genetic information. Philos Trans R Soc Lond B Biol Sci. 358:87–97.

Herrmann RG, Possingham JV. 1980. Plastid DNA—the plastome. In: Reinert J, editor. Results and problems in cell differentiation. Berlin (Germany): Springer. p. 45–96.

Herrmann RG, Seyer P, Schedel R, et al. 1980. (11 co-authors). 1980. The plastid chromosomes of several dicotyledons. In: Bücher T, Sebald W, Weiß H, editors. Biological chemistry of organelle formation. Berlin (Germany): Springer. p. 97–112.

Herrmann RG, Westhoff P. 2001. Thylakoid biogenesis: the result of a complex phylogenetic puzzle. In: Aro E-M, Andersson B, editors. Regulation of photosynthesis. Dordrecht (The Netherlands): Kluwer Academic Publishing. p. 1–28.

Homann A, Link G. 2003. DNA-binding and transcription characteristics of three cloned sigma factors from mustard (*Sinapis alba* L.) suggest overlapping and distinct roles in plastid gene expression. Eur J Biochem. 270:1288–1300.

Kanamaru K, Tanaka K. 2004. Roles of chloroplast RNA polymerase sigma factors in chloroplast development and stress response in higher plants. Biosci Biotechnol Biochem. 68:2215–2223.

Kapoor S, Sugiura M. 1999. Identification of two essential sequence elements in the nonconsensus type II PatpB-290 plastid promoter by using plastid transcription extracts from cultured tobacco BY-2 cells. Plant Cell. 11:1799–1810.

Kapralov MV, Filatov DA. 2007. Widespread positive selection in the photosynthetic Rubisco enzyme. BMC Evol Biol. 7:73.

Klughammer C, Schreiber U. 1998. Measuring P700 absorbance changes in the near infrared spectral region with a dual wavelength pulse modulation system. In: Garab G, editor. Photosynthesis: mechanisms and effects. Dordrecht (The Netherlands): Kluwer Academic Publishers. p. 4357–4360.

Kofer W, Koop HU, Wanner G, Steinmüller K. 1998. Mutagenesis of the genes encoding subunits A, C, H, I, J and K of the plastid NAD(P)H-plastoquinone-oxidoreductase in tobacco by polyethylene glycol-mediated plastome transformation. Mol Gen Genet. 258:166–173.

Kooten O, Snel JFH. 1990. The use of chlorophyll fluorescence nomenclature in plant stress physiology. Photosynth Res. 25:147–150.

Levin DA. 2003. The cytoplasmic factor in plant speciation. Syst Bot. 28:5–11.

Levin RA, Wagner WL, Hoch PC, Hahn WJ, Rodriguez A, Baum DA, Katinas L, Zimmer EA, Sytsma KJ. 2004. Paraphyly in tribe *Onagreae*: insights into phylogenetic relationships of *Onagraceae* based on nuclear and chloroplast sequence data. Syst Bot. 29:147–164.

Levin RA, Wagner WL, Hoch PC, Nepokroff M, Pires JC, Zimmer EA, Sytsma KJ. 2003. Family-level relationships of *Onagraceae* based on chloroplast rbcL and ndhF data. Am J Bot. 90:107–115.

Liere K, Börner T. 2006. Transcription of plastid genes. In: Grasser KD, editor. Regulation of transcription in plants. Oxford: Backwell Publishing. p. 184–233.

Martin W. 2003. Gene transfer from organelles to the nucleus: frequent and in big chunks. Proc Natl Acad Sci USA. 100:8612–8614.

Martin W, Stoebe B, Goremykin V, Hapsmann S, Hasegawa M, Kowallik KV. 1998. Gene transfer to the nucleus and the evolution of chloroplasts. Nature. 393:162–165.

Meurer J, Lezhneva L, Amann K, Gödel M, Bezhani S, Sherameti I, Oelmüller R. 2002. A peptide chain release factor 2 affects the stability of UGA-containing transcripts in *Arabidopsis* chloroplasts. Plant Cell. 14:3255–3269.

Meurer J, Meierhoff K, Westhoff P. 1996. Isolation of high-chlorophyll-fluorescence mutants of *Arabidopsis thaliana* and their characterisation by spectroscopy, immunoblotting and northern hybridisation. Planta. 198:385–396.

Mráček J, Greiner S, Cho WK, et al. (16 co-authors). 2006. Construction, database integration, and application of an *Oenothera* EST library. Genomics. 88:372–380.

Neckermann K, Zeltz P, Igloi GL, Kossel H, Maier RM. 1994. The role of RNA editing in conservation of start codons in chloroplast genomes. Gene. 146:177–182.

Raven PH. 1988. *Onagraceae* as a model of plant evolution. In: Gottlieb LD, Jain SK, editors. Plant evolutionary biology: a symposium honouring G. Ledyard Stebbins. London: Chapman and Hall. p. 85–107.

Renner O. 1934. Die pflanzlichen Plastiden als selbständige Elemente der genetischen Konstitution. Ber Math Phys Kl Sächs Akad Wiss Leipzig. 86:241–266.

Schmitz-Linneweber C, Kushnir S, Babiychuk E, Poltnigg P, Herrmann RG, Maier RM. 2005. Pigment deficiency in nightshade/tobacco cybrids is caused by the failure to edit the plastid ATPase alpha-subunit mRNA. Plant Cell. 17: 1815–1828.

Schmitz-Linneweber C, Regel R, Du TG, Hupfer H, Herrmann RG, Maier RM. 2002. The plastid chromosome of *Atropa belladonna* and its comparison with that of *Nicotiana tabacum*: the role of RNA editing in generating divergence in the process of plant speciation. Mol Biol Evol. 19:1602–1612.

Schmitz-Linneweber C, Tillich M, Herrmann RG, Maier RM. 2001. Heterologous, splicing-dependent RNA editing in chloroplasts: allotetraploidy provides trans-factors. EMBO J. 20:4874–4883.

Schreiber U, Bilger W, Hormann H, Neubauer C. 1998. Chlorophyll fluorescence as a diagnostic tool: basics and some aspects of practical relevance. In: Rughavendra AS, editor. Photosynthesis: a comprehensive treatise. Cambridge: Cambridge University Press. p. 320–336.

Schwenkert S, Umate P, Dal Bosco C, Volz S, Mlçochová L, Zoryan M, Eichacker LA, Ohad I, Herrmann RG, Meurer J. 2006. PsbI affects the stability, function, and phosphorylation patterns of photosystem II assemblies in tobacco. J Biol Chem. 281:34227–34238.

Shiina T, Tsunoyama Y, Nakahira Y, Khan MS. 2005. Plastid RNA polymerases, promoters, and transcription regulators in higher plants. Int Rev Cytol. 244:1–68.

Shikanai T. 2006. RNA editing in plant organelles: machinery, physiological function and evolution. Cell Mol Life Sci. 63:698–708.

Silhavy D, Maliga P. 1998. Mapping of promoters for the nucleus-encoded plastid RNA polymerase (NEP) in the iojap maize mutant. Curr Genet. 33:340–344.

Sriraman P, Silhavy D, Maliga P. 1998. The phage-type PclpP-53 plastid promoter comprises sequences downstream of the transcription initiation site. Nucleic Acids Res. 26:4874–4879.

Steiner EE, Stubbe W. 1984. A contribution to the population biology of *Oenothera grandiflora* L'Her. Am J Bot. 71: 1293–1301.

Stubbe W. 1963. Extrem disharmonische Genom-Plastom-Kombinationen und väterliche Plastidenvererbung bei *Oenothera*. Z Vererbungsl. 94:392–411.

Stubbe W. 1964. The role of the plastome in evolution of the genus *Oenothera*. Genetica. 35:28–33.

Stubbe W. 1989. *Oenothera*—an ideal system for studying the interaction of genome and plastome. Plant Mol Biol Rep. 7:245–257.

Stubbe W, Pietsch B, Kowallik KV. 1978. Cytologische Untersuchungen über väterliche Plastidenvererbung und plastomabhängige Degradation der Samenanlagen bei einem *Oenothera*-Bastard. Biol Zentralbl. 97:39–52.

Stubbe W, Raven PH. 1979. A genetic contribution to the taxonomy of *Oenothera* sect. *Oenothera* (including

subsection *Euoenothera*, *Emersonia*, *Raimannia* and *Munzia*). Plant Syst Evol. 133:39–59.
Swiatecka-Hagenbruch M, Liere K, Börner T. 2007. High diversity of plastidial promoters in *Arabidopsis thaliana*. Mol Genet Genomics. 277:725–734.
Tillich M, Funk HT, Schmitz-Linneweber C, Poltnigg P, Sabater B, Martin M, Maier RM. 2005. Editing of plastid RNA in *Arabidopsis thaliana* ecotypes. Plant J. 43:708–715.
Tsudzuki T, Wakasugi T, Sugiura M. 2001. Comparative analysis of RNA editing sites in higher plant chloroplasts. J Mol Evol. 53:327–332.
Westhoff P. 1985. Transcription of the gene encoding the 51 kd chlorophyll a-apoprotein of the photosystem II reaction centre from spinach. Mol Gen Genet. 201:115–123.
Westhoff P, Herrmann RG. 1988. Complex RNA maturation in chloroplasts. The psbB operon from spinach. Eur J Biochem. 171:551–564.
Yang Z. 1997. PAML: a program package for phylogenetic analysis by maximum likelihood. Comput Appl Biosci. 13:555–556.

Franz Lang, Associate Editor

Accepted July 1, 2008